JPL Publication 00-19

Results of the 2000 JPL Balloon Flight Solar Cell Calibration Program

B. E. Anspaugh
R. L. Mueller
R. S. Weiss

National Aeronautics and Space Administration

Jet Propulsion Laboratory
California Institute of Technology
Pasadena, California

February 1, 2001

JPL Publication 00-19

Results of the 2000 JPL Balloon Flight Solar Cell Calibration Program

B. E. Anspaugh
R. L. Mueller
R. S. Weiss

National Aeronautics and Space Administration

Jet Propulsion Laboratory
California Institute of Technology
Pasadena, California

February 1, 2001

This research was carried out at the Jet Propulsion Laboratory, California Institute of Technology, under a contract with the National Aeronautics and Space Administration.

ABSTRACT

The 2000 solar cell calibration balloon flight campaign consisted of two flights, which occurred on June 27, 2000, and July 5, 2000. All objectives of the flight program were met. Sixty-two modules were carried to an altitude of $\approx$ 120,000 ft (36.6 km). Full I-V curves were measured on sixteen of these modules, and output at a fixed load was measured on thirty-seven modules (forty-six cells), with some modules repeated on the second flight. Nine modules were flown for temperature measurement only. This data was corrected to 28°C and to 1 AU (1.496×10^8 km). The calibrated cells have been returned to their owners and can now be used as reference standards in simulator testing of cells and arrays.

ACKNOWLEDGMENTS

The authors wish to express appreciation for the cooperation and support provided by the entire staff of the National Scientific Balloon Facility located at Palestine, Texas. Matt Tuchscherer of JPL was very helpful in preparing the system for flight. The strong programmatic support from Perry Bankston, Steve Marroquin, and Julie Selders of JPL and from Ruth Netting and Robert Hayduk of NASA Headquarters is deeply appreciated.

CONTENTS

Figures

Tables

"Anyone who has never made a mistake has never tried anything new." *Albert Einstein*

1. INTRODUCTION AND OVERVIEW

The primary source of electrical power for robotic space vehicles is the direct conversion of solar energy through the use of solar cells. As advancing cell technology continues to modify the spectral response of solar cells to utilize more of the Sun's spectrum, designers of solar cells and arrays must have the capability of measuring these cells in a light beam that is a close match to the solar spectrum. The solar spectrum has been matched closely by laboratory solar simulators. But the design of solar cells and the sizing of solar arrays require such highly accurate measurements that the intensity of these simulators must be set very accurately. A small error in setting the simulator intensity can conceivably cause a disastrous missizing of a solar panel, causing either a premature shortfall in power or the launch of an oversized, overweight solar panel.

The Jet Propulsion Laboratory (JPL) solar cell calibration program was conceived to produce reference standards for the purpose of accurately setting solar simulator intensities. The concept is to fly solar cells on a high-altitude balloon, to measure their output at altitudes near 120,000 ft (36.6 km), to recover the cells, and to use them as reference standards for setting solar simulator intensities. This is done by placing the reference cell in the simulator beam, then adjusting the beam intensity until the reference cell reads the same as it read on the balloon. As long as the reference cell has the same spectral response as the cells or panels to be measured, this is a very accurate method of setting the intensity. But as solar cell technology changes, the spectral response of the solar cells changes also, and reference standards using the new technology must be built and calibrated.

Until the summer of 1985, there had always been a question as to how much the atmosphere above the balloon modified the solar spectrum. If the modification was significant, the reference cells might not have the required accuracy. Solar cells made in recent years have increasingly higher blue responses; if the atmosphere has any effect at all, it would be expected to modify the calibration of these newer blue cells much more than for cells made in the past.

In late 1984, a collection of solar cells representing a wide cross section of solar cell technology was flown on the shuttle Discovery as a part of the Solar Cell Calibration Facility (SCCF) experiment. The cells were calibrated as reference cells on this flight by using procedures similar to those used on the balloon flights. The same cells were then flown on the 1985 balloon flight and remeasured. The 2 sets of measurements gave nearly identical results (see reference 1), thus verifying the accuracy of the calibration procedures used on the balloon flights.

JPL has been flying calibration standards on high-altitude balloons since 1963 and continues to organize a calibration balloon flight at least once a year. The 2000 balloon flights were the 57th and 58th flights in the series. The 2000 flights incorporated a total of 62 solar cell modules. There was a total of 9 different participants, including JPL. The payload included Si, GaAs, GaAs/Ge, Ge, and multi-junction cells, along with top and bottom sections of dual and triple-junction cells.

A new data acquisition system was built for the balloon flights and flown for the first time on the 1995 flight. This system allows the measurement of current-voltage (I-V) curves for 19 modules, in addition to measurement of modules with fixed loads, as had been done in the past.

The Sun angle sensor, first flown in 1997, was flown on the 2000 flights. This sensor measures the angle of the Sun in both azimuth and elevation and adds this information to the telemetry stream using 4 of the fixed-cell data channels.

2. PREFLIGHT PROCEDURES

2.1 MODULE FABRICATION

The cells were mounted by the participants or by JPL on JPL-supplied standard modules in accordance with standard procedures developed for the construction of reference cells. The JPL standard module is a machined copper or aluminum block on which a fiberglass circuit board is mounted. The circuit board has terminals that are used for making electrical connections to the solar cell

and to a load resistor. On those cells slated for I-V measurement, no load resistor is connected. The circuit boards include 2 binding posts and a jumper in series with one of the leads to the resistor. After flight calibration, the jumper can be removed and replaced with current pickoff probes for use on those pulsed xenon simulators that require a current input. The cell current (mA) will then be equal to the cell calibration value (mV) divided by the load resistance. The assembly is painted with either high-reflectance white or low-reflectance black paint.

The resistor on the fixed-load cells performs 2 tasks. First, it loads the cells near short-circuit current (I_{sc}), which is the cell parameter that varies in direct proportion to light intensity. Second, it scales the cell outputs to read slightly less than 100 mV during the flight, the maximum input voltage allowed by the data acquisition electronics for the fixed-load cells. Load resistance values are chosen to match the electrical characteristics of each cell flown. Nominally, the resistors will be $\approx$0.5 ohm for a 2 x 2 cm Si cell, 0.66 ohm for a 2 $\times$ 2 cm GaAs cell, 0.25 ohm for a 2 $\times$ 4 cm Si cell, etc. The load resistors are precision resistors (1.0%, 20 ppm/°C) and have a resistance stability equal to or better than $\pm$0.002% over a 3-year period. The solar cells are permanently glued to the body of the machined metal block with RTV 560 or its equivalent. This gives a good thermal conductivity path between the cells and the metal blocks, while providing electrical insulation between the rear surface of the solar cells and the block.

2.2 CELL MEASUREMENTS

After the cells were mounted on the blocks, the electrical output of each cell module was measured under illumination by the JPL X25 Mark II solar simulator. For these measurements, the simulator intensity was set by using only one reference cell—no attempt was made to match the spectral response of the reference standard to the individual cell modules. The absolute accuracy of these measurements is therefore unknown, but the measurements do allow checking of the modules for any unacceptable assembly losses or instabilities. After the balloon flight, the cells were measured in exactly the same way to check for any cell damage or instabilities that may have occurred as a result of the flight.

2.3 TEMPERATURE COEFFICIENTS AND LEAST SQUARES FITS

The temperature coefficients of the mounted cells were also measured before the flight. The modules were mounted in their flight configuration on a temperature-controlled block in a vacuum chamber. Cell outputs were measured at 25, 35, 45, 55, 65, and 75°C under illumination with the X25 simulator. The temperature coefficients of the fixed-cell cell modules were computed by fitting the output vs. temperature relationship with a linear least squares fit. Temperature coefficients for the I-V cells were computed using a linear least squares fit to both the short-circuit current and open-circuit voltage (V_{oc}) data.

The data analysis program was modified in 1998 to allow the measurement of cell temperature coefficients using the flight data. When the tracker first locks on the Sun after reaching float altitude during the flight, the cell temperatures are $\approx$40°C. As the flight progresses, the cell temperatures rise to $\approx$75°C. This data was used to compute temperature coefficients both for the fixed-load cells and for the I-V cells. In the latter case, temperature coefficients for both I_{sc} and V_{oc} were computed. The temperature coefficients measured during the flight were compared with those measured with the X25, and those that seemed to give the best fits to the data were used for the analysis.

2.4 DATA ACQUISITION SYSTEM CHECKOUT AND CALIBRATION

The 1995 data acquisition (DAQ) system was used for the calibration measurements on the 2000 flights. This system is based on a 286 microprocessor in a ROM-DOS operating system. The program that controls the system is easily changed to match the requirements of each individual flight. This system also duplicates the function of the older data encoder with regard to reading and processing the outputs of the modules with fixed-load resistors (maximum input voltage of 100 mV). The system has 7 dedicated temperature measurement channels, 6 for the panel and 1 for the internal DAQ temperature. The temperature sensors are now platinum resistance sensors (RTDs) instead of the thermistors that were used in the older encoder. The system has the capability of measuring the I-V characteristics of as many as 19 solar cells and one reference channel. Loading of the cells to produce the I-V curves is accomplished by applying 20 resistive loads, one at a time, to each cell and measuring the cell's output voltage and current as each load is applied. Each cell has its own individually tailored set of 20 load resistors. The resistive loads are chosen to generate the expected I-V characteristic of each cell and to produce a large number of points near the maximum power (P_{max}) point. Sixteen resistors are available for cell loading. Selection of these resistors in parallel combinations of up to 5 at a time results in a theoretical total of 6,884 possible resistive loads (although this number includes many duplicates) available for each

cell. A 4-wire system is used for the I-V measurements, so that the wires measuring cell voltage do not carry current.

The heart of the DAQ is a 286-class computer on an STD bus circuit board. This computer controls the multiplexing of the cells data, temperature data, calibration voltages, and power supply voltages for measurement. The computer is also used to connect each I-V cell in its turn to the measurement circuitry, and the computer also applies the tailored set of load resistors across the cell under measurement. The computer is used to format the data, to add clock time, synch words, and a checksum for each line, and then to send all of this to the telemetry transmitter via an RS232 output at a rate of 9600 baud. All of the test and measurement parameters are read out and transmitted during the course of a telemetry frame. During this time the fixed-load cells are each read 5 times, and each of the I-V cells is read once. All other engineering voltages and temperatures are also read once each frame. As presently programmed, a telemetry frame is sent every 9.5 seconds.

All measurements of electrical parameters are performed by sending the signals through suitable amplifiers, and then to a 12-bit A/D converter. The fixed-load cell signals are sent through an amplifier with a gain of 49.7858. The I-V cell voltage levels are sent through an amplifier with a gain of 1.7662. (Note: This amplifier was decreased from its previous value of 2.0 to accommodate the higher open-circuit voltages produced by modern dual- and triple-junction cells.) Cell currents were passed through a precision 0.1-ohm resistor. The voltage drop across this resistor was fed to a differential amplifier with a system (resistor plus amplifier) gain of 5.2728 volts/amp. These gains were measured by connecting a series of voltages (or currents) into the multiplexer feeding each amplifier and measuring the output voltage. These gains are measured each year either before or after the flight(s). The repeatability of the gain measurements to date has been better than 0.03% for the voltage amplifiers and better than 0.17% for the current amplifier. The on-Sun indicator and the 7 temperature signals were each sent through individual amplifiers. These amplifiers were also individually calibrated prior to flight. Calibration voltages were built into the DAQ and are used for monitoring the gain and stability of the voltage amplifiers during the flight. Three calibration voltages of approximately 50, 80, and 100 mV from an external voltage reference box are also multiplexed into the data stream as a cross-check on the system. The Sun-angle-sensor data was sent through 4 of the fixed-load channels and incorporated into the telemetry stream.

The program was modified in 1999 to calculate the gain of the fixed-load-cell amplifier continuously during the flight. The known, stable voltages from the external voltage reference source were used as input, and the telemetered output values were used as output. A linear least squares fit routine was used to calculate the gain and offset of the amplifier continuously during the flight.

The program was again modified in 2000 to allow the option of calculating the gain of the fixed-load-cell amplifier using internal calibration voltages of ≈ 50 and 90 mV built into the DAQ. This option also permits calculating the gain and offset of the amplifier continuously during the flight.

The system is designed so that the output from the DAQ on the RS232 line can be fed directly to the COM input of a PC for preflight testing. During the flight, the line connecting the RS232 output to the PC is replaced with connections to a telemetry transmitter and a telemetry receiver. Since the overall system operation is equally effective whether the connection is by cable or by radio, this configuration allows a much more thorough checkout of the system before it leaves JPL and during the various preflight checkouts at the National Scientific Balloon Facility (NSBF) at Palestine, Texas.

The PC program for receiving, converting, and storing data is written in LabVIEW, a graphical programming language specifically designed for making engineering-type measurements under PC control. The LabVIEW program provides for graphical display of the outputs from all the fixed-load cells simultaneously. The I-V curves of any or all of the 19 I-V cells may also be displayed. The program provides for digital readout of all power supply voltages, calibration voltages, temperatures, and on-Sun indicator readings. The Sun-angle-sensor data is displayed in the form of a scatter plot on the LabVIEW display. Synch status and checksum status are continuously displayed. These displays are continuously updated in real time and give an instantaneous reading on the status of the whole system.

2.5 PANEL ASSEMBLY AND CHECKOUT

After the electrical measurements of the solar cells were completed, the modules were mounted on the solar panel and connected electrically. Figure 1 is a photograph of the mounted modules for the first 2000 flight, Figure 2 is a diagram of the panel that identifies the modules by their serial numbers, and Figure 3 is a photograph of the tracker and panel after it was later mounted on the hoop assembly at Palestine. Figures 4, 5, and 6 show similar views of the assemblies for the second

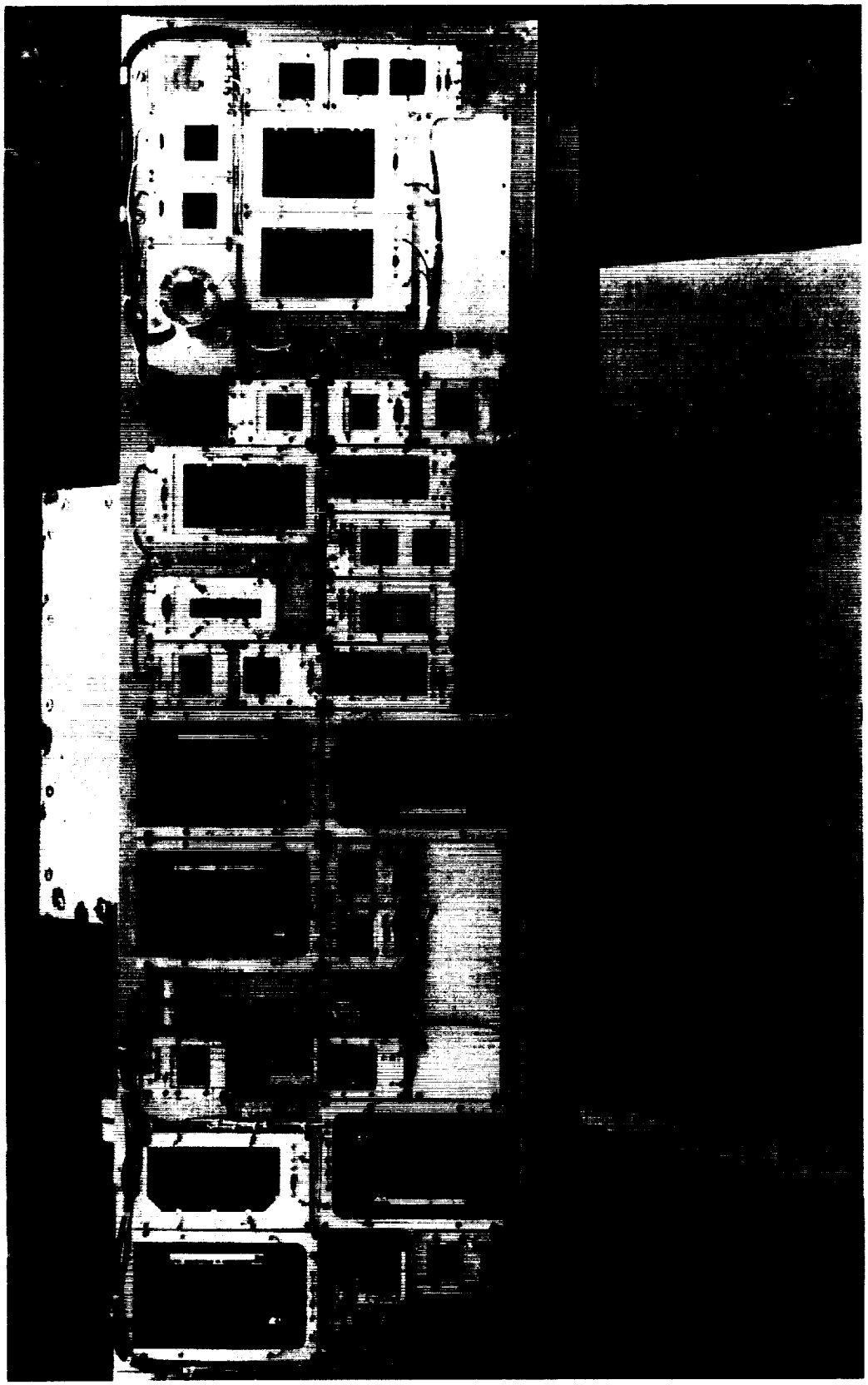

Figure 1. Photograph of the 2000-1 Balloon Flight Solar Panel

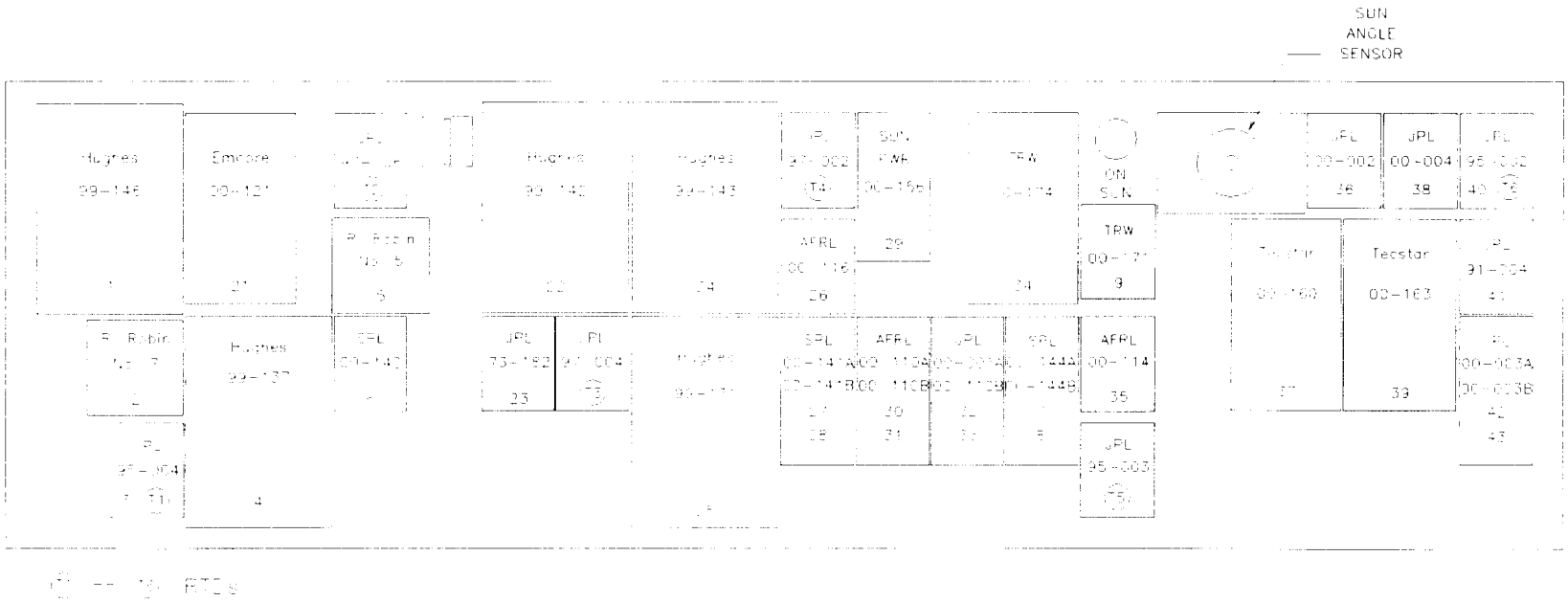

Figure 2. Module Location Chart, 2000-1 Flight

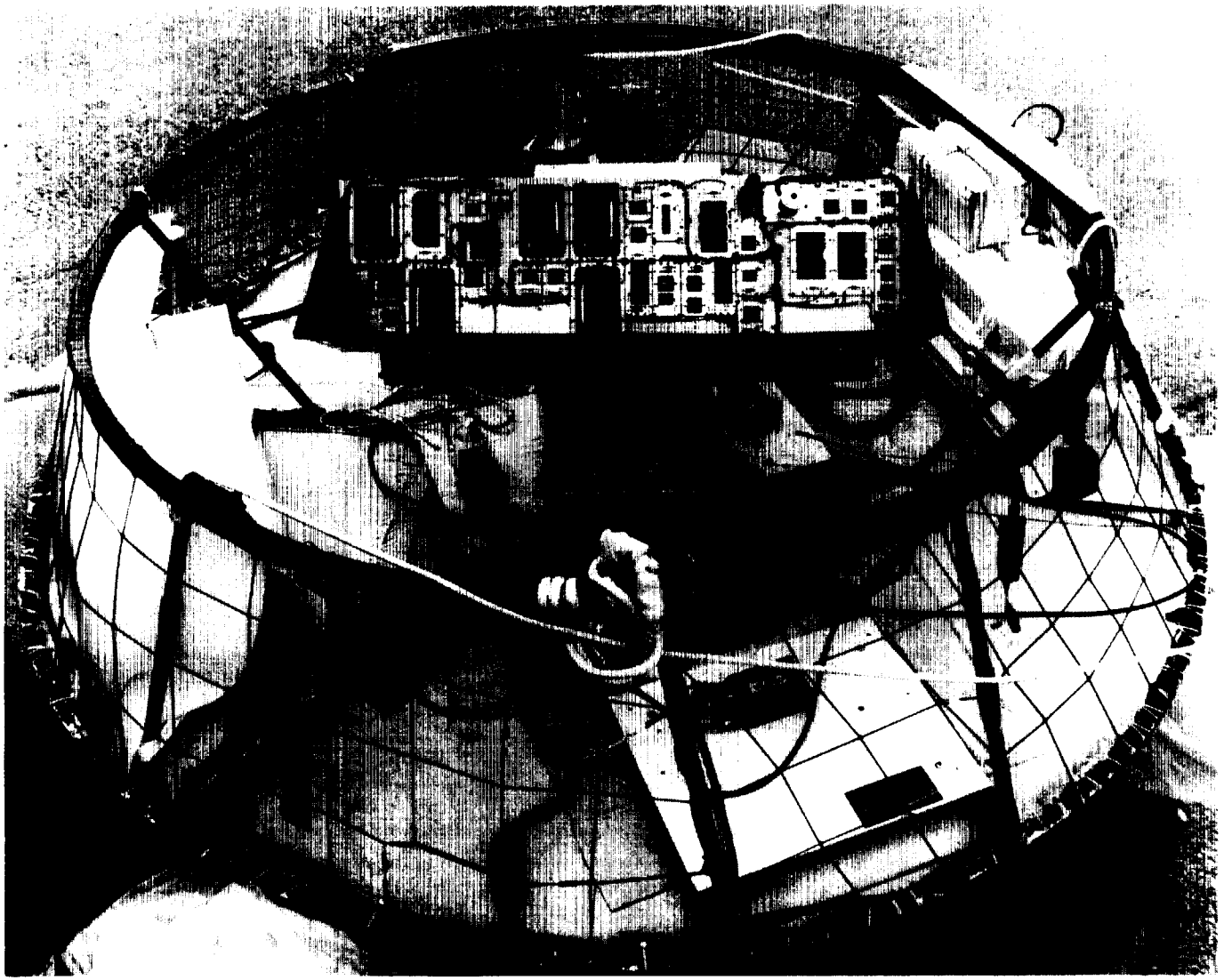

Figure 3. Tracker Mounted on Aluminum Hoop Assembly for 2000-1 Flight

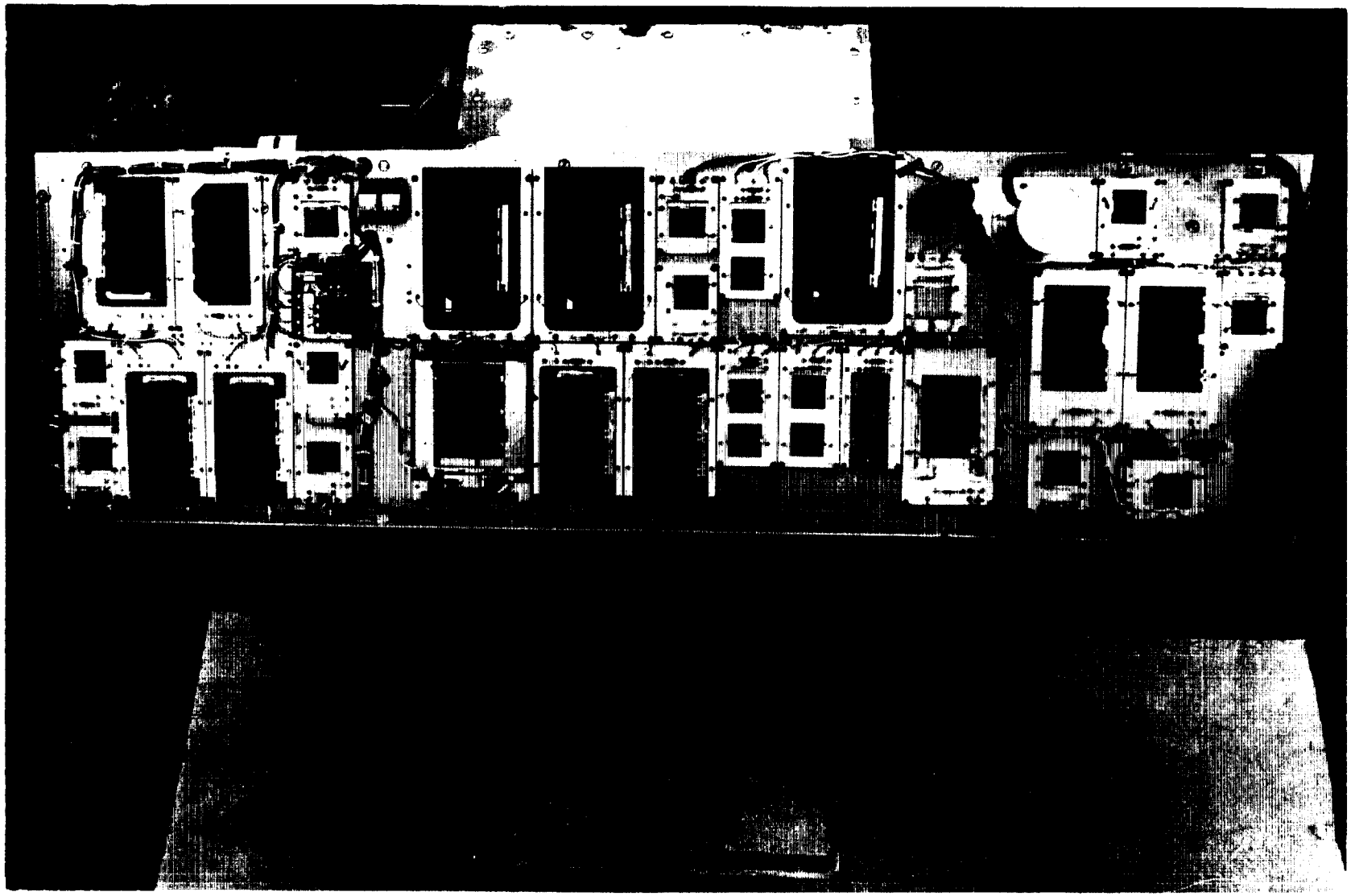

Figure 4. Photograph of the 2000-2 Balloon Flight Solar Panel

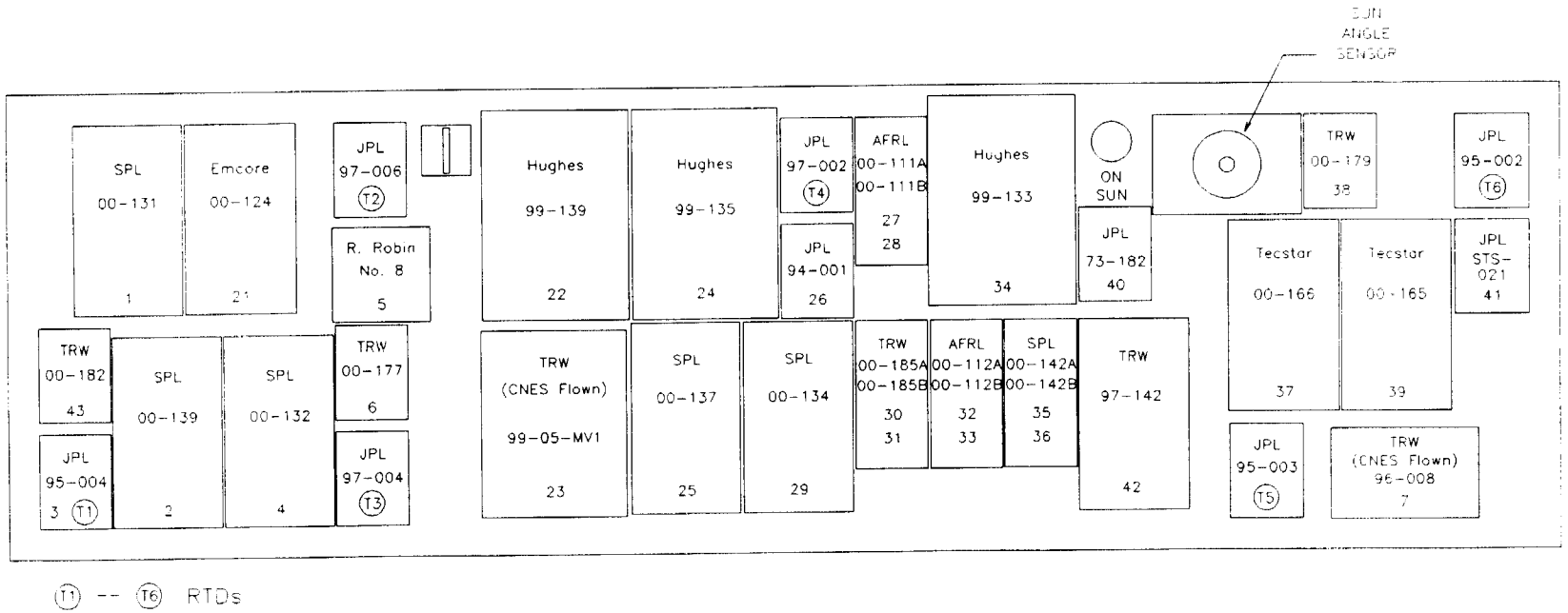

Figure 5. Module Location Chart, 2000-2 Flight

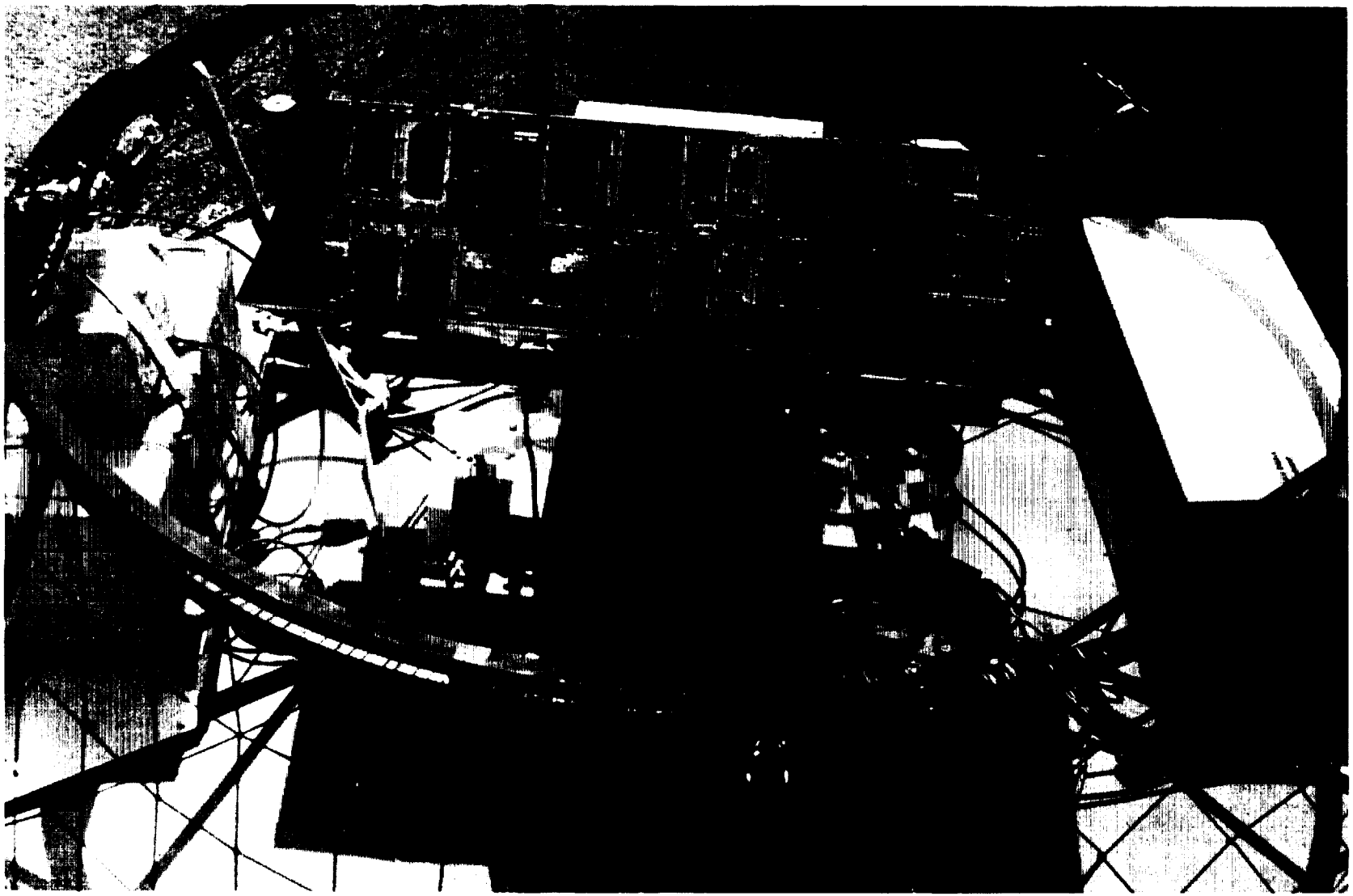

Figure 6. Tracker Mounted on Aluminum Hoop Assembly for 2000-2 Flight

2000 flight. After completion of the panel assembly, the panel, tracker, and DAQ were all given complete functional tests in terrestrial sunlight. The assembled tracker and panel were placed in sunlight on a clear, bright day and checked for the tracker's ability to acquire and track the Sun while each cell module was checked for electrical output. All power supply voltages and temperature readings were checked, and the calibration voltages were checked for stability and proper function. After these tests were completed satisfactorily, the assembly was shipped to NSBF for flight.

2.6 PRELAUNCH PROCEDURES AT PALESTINE

The NSBF was established in 1963 at Palestine, Texas. This location was chosen because it has favorable weather conditions for balloon launching and a large number of clear days with light surface winds. The JPL calibration flights have flown from the Palestine facility since 1973. The flights are usually scheduled in the June-to-September time period, since the Sun is high in the sky at that time of year and the sunlight passes through a minimum depth of atmosphere before reaching the solar modules. Also, the high-altitude winds in this time period take the balloons over the sparsely populated areas of east-Texas, so the descending payloads are unlikely to cause damage to persons or property.

Upon arrival at Palestine, the tracker and module payload were again checked for proper operation. This included a checkout in an environmental test chamber wherein the tracker, calibration voltages, and the entire data acquisition system were all tested as a system. The chamber was pumped down to a pressure of ≈ 5 mbar (0.05 N/cm^2), then backfilled with dry nitrogen to a pressure of ≈ 800 mb. The DAQ was then cooled to $-40°$C. The system was tested at 10° increments during the cooldown. The system was pumped down to a pressure of 5 mbar (corresponding to an altitude of 118,000 ft) and soaked for 30 minutes at this temperature and pressure. Following this, the chamber was backfilled with dry nitrogen and warmed up to $+50°$C, with tests occurring at each 10° increment. Then the assembly was removed from the environmental chamber, and a room-temperature, end-to-end check was performed on the payload, telemetry, receiving, and decoding systems.

After all the checkouts and calibrations were performed, the tracker was mounted on an aluminum tubular hoop structure. This assembly was then mounted on the top portion (or apex) of the balloon. Figures 3 and 6 are photographs of the tracker mounted on the hoop assembly for the first and second 2000 flights. The solar panel is shown as it was configured for the 2 flights.

3. BALLOON SYSTEM

The main components of the balloon flight system are (1) the apex-mounted hoop assembly that contains the experimental package, the data encoder, the command receiver, the data telemetry system, and the recovery system; (2) the balloon; and (3) the lower payload that contains the terminate system, the Global Positioning System (GPS) receivers, transponder, and the housekeeping telemetry system and command receiver for the balloon system. There was a major change in the design of the balloon system in 1997. A special telemetry system was designed specifically for the top payload. This system consists of a command receiver, data telemetry transmitter, and a transmitter for sending housekeeping data for the top payload. These items, along with the batteries to power them, are all installed on the hoop assembly. The main balloon system has its own command receivers and telemetry transmitters as before, but the two systems are now completely isolated from each other. This new design was implemented in order to eliminate the long cables running from the top of the balloon to the systems at the bottom gondola, as it was suspected that these long cables behaved like antennas capable of picking up electrostatic charges and inducing flight failures.

A color TV camera was added to the top payload assembly in 1998. This camera, along with its dedicated transmitter and battery supply, allows the team to view the operation of the tracker in real time during the flight. The images are recorded on a VCR in the NSBF control tower for later viewing.

3.1 BALLOON DESCRIPTION

The balloons used for the JPL solar cell calibration high-altitude flights are manufactured by the Winzen Balloon Group of Raven Industries. The balloons have a volume of 3.46 million ft^3 (98,000 m^3). The balloon manufacturer uses 0.8-mil (20-μm) polyethylene film (Stratofilm-372) designed specifically for balloon use. The balloon alone weighs 702 lb (319 kg). It is designed to lift itself and a payload weight of up to 725 lb (330 kg), distributed between the bottom and top payloads, to a float altitude of 120,000 ft (36.6 km). At float altitude, the balloon has a diameter of roughly 213 ft (65 m) and a height of 146 ft (45 m). The balloon is built with an internal rip line designed to rip a hole in the side of the balloon for termination of the flight. A special structure is built into the top of the balloon for attaching the top payload. The payload is attached to this structure by means of a stainless steel cable. At flight termination

time, a command is sent to cut the cable, allowing the payload to fall away from the balloon.

Trying to inflate and launch a balloon with a sizable weight attached to its top is very awkward and may be likened to trying to fend off a grizzly bear with a broom stick. A tow balloon tied to the top payload was used during the inflation and launch phases to add stability and to keep it on top. This smaller balloon, about 2,900 ft^3 (82 m^3), is designed to lift about 180 lb (82 kg). The tow balloon was cut loose from the top payload after the launch as soon as the main balloon stabilized and the launch-induced oscillations damped out.

3.2 TOP PAYLOAD

The top payload consists of the tracker, solar panel, voltage reference box, multiplexer, data encoder, descent parachute, relay box, tracking beacons, telemetry transmitters, command receivers, television camera, and battery power supplies for the tracker, data encoder, receiver, and transmitters. All these items are mounted on the aluminum hoop assembly as shown in Figures 3 and 6. The hoop assembly also serves the following functions:

(1) Permits the top-mounted payload to "float" on top of the balloon and minimizes billowing of balloon material around the top payload.

(2) Serves as the mounting surface that attaches the top payload assembly to the balloon.

(3) Provides a convenient point for attaching the tow balloon and the descent parachute.

(4) Acts as a shock damper to protect and minimize damage to the top payload at touchdown.

The complete apex-mounted hoop assembly, as flown, weighs $\approx$ 140 lb (63 kg) and descends as a unit by parachute at flight termination.

The Sun tracker, shown in Figures 3 and 6, is capable of orienting the solar panel toward the Sun, compensating for the motion of the balloon and the Sun by using 2-axis tracking in both azimuth and elevation. The tracker has the capability to maintain its lock on the Sun to within ± 1 deg. To verify that the tracker was operating properly, the output of an on-Sun indicator was constantly monitored during the flight by feeding its output to the DAQ and entering its signal into the telemetry stream. The on-Sun indicator consists of a small, circular solar cell mounted at the bottom of a collimator tube, 7 in. (17.8 cm) long, with an aperture measuring 0.315 in. (0.8 cm) in diameter. The on-Sun indicator is attached to the solar panel so that it points at the Sun when the panel is perpendicular to the Sun. The output of the on-Sun indicator falls off very rapidly as the collimator tube points away from the Sun and provides a very sensitive indication of proper tracker operation. A Sun-angle-sensor, added to the system in 1996, gives a quantitative readout of the tracker's pointing accuracy.

A reflection shield is attached to the panel to prevent any stray reflected light from reaching any of the modules. This shield is made of sheet aluminum, painted black, and attached to 3 edges of the solar panel.

For the first 2000 flight, the solar cell modules were mounted onto the Sun tracker platform with an interface of Apiezon H vacuum grease and held in place with 4 screws. The grease is used to achieve a highly conductive thermal contact between the modules and the panel and to smooth out the temperature distribution over the solar panel as much as possible. For the second 2000 flight, a thermal interface of crinkled aluminum foil was used in place of the Apiezon grease. We have used the foil for thermal interfacing in our laboratory vacuum systems for several years with good results, and the results proved equally satisfactory during this flight. This procedure eliminates the mess associated with the grease.

The solar panel temperature is monitored using platinum resistance sensors (RTDs). Some of the solar cell modules are constructed with RTDs embedded in the metal substrate directly beneath the solar cell. Six of these modules are mounted on the solar panel at equally spaced locations so that their temperature readings give an accurate representation of panel temperature. Placement of these modules on the 2 flight panels is shown in Figures 2 and 5. A seventh RTD is mounted inside the DAQ to monitor its temperature during environmental testing and during the flight.

A tracking or locator beacon was attached to the hoop assembly. This beacon, similar to those used for tracking wild animals in their natural habitat, consists of a low-wattage transmitter that sends short, 168-MHz pulses at the rate of about 1 per second. A handheld directional antenna and a battery-powered receiver are used inside the chase plane and on the ground for locating the transmitter. This beacon has been very useful in locating this very small payload in a very large open range.

3.3 BOTTOM PAYLOAD

The bottom payload was entirely furnished by the NSBF. It consists of a battery power supply, a ballast module for balloon control, a terminate package, and an electronics module known as the consolidated instrument package (CIP).

Power for operating most of the electrical and electronic equipment on the balloon is supplied by a complement of high-capacity lithium batteries. This supply, furnishing 28 Vdc regulated power and 36 Vdc unregulated power, powered all the instruments in the CIP. Several other small battery sources were used at various locations on the balloon for instruments that require small amounts of power. For example, the tracker and data encoder, the tracking beacons, the voltage reference box, and the payload telemetry system all have individual battery power supplies. All batteries are sized to supply power for at least twice the expected duration of a normal flight.

High-altitude balloons tend to lose helium slowly during the course of the flight. As a consequence, a helium balloon will tend to reach float altitude and then begin a slow descent. To counteract this tendency, a ballast system is included as part of the bottom payload. It usually contains $\approx$100 lb (45 kg) of ballast in the form of very fine steel shot. The shot may be released in any desired amount by radio command. By proper use of this system, float altitude may be maintained to within $\pm$2,000 ft ($\pm$600 m).

The telemetry system in the CIP sends all data transmissions concerning the flight except those for the top payload over a common RF carrier. The CIP also contains a command system for sending commands to the balloon for controlling the housekeeping functions such as releasing ballast and turning the transponder on and off. Specifically, the CIP contains the following equipment:

(1) Pressure transducers
(2) Subcarrier oscillators, as required
(3) An L-band FM transmitter
(4) A transponder for air traffic control tracking
(5) A pulse code modulation (PCM) command receiver-decoder
(6) Two GPS receivers

The altitude of the balloon is measured with a capacitance-type electronic transducer, manufactured by MKS Instruments, Inc., which reads pressure within the range of 1,020 to 0.4 mbar (102,000 to 40 N/m^2) with an accuracy of 0.05%. The transducer produces a dc level that is encoded as PCM data and decoded at the receiving station into pressure, and the altitude is then calculated from the pressure reading. The GPS receivers also compute and send altitude information into the telemetry stream.

The GPS navigation system is used for flight tracking. The second GPS receiver is used as a backup. This system can provide position data to an uncertainty of less than 0.1 mi (0.2 km). The GPS signal is multiplexed into the telemetry stream and updated every 8 seconds.

All the telemetry data is sent to the ground in the form of pulse code modulation. A UHF L-band transmitter in the CIP is used to generate the RF carrier. The L-band carrier is modulated by the pulse code and sent to the receiving station at Palestine.

An aircraft-type transponder is flown so that Air Traffic Control (ATC) could read the balloon's location on their radar systems during the descent portion of the flight. ATC is often helpful in relaying to the recovery aircraft the exact position of the bottom payload during its descent on the parachute.

The purpose of the PCM command systems is to send commands to the balloon; e.g., release the bottom payload from the balloon and release ballast. Like the PCM system used on the top payload, it is designed to reject false commands and is highly reliable in operation. The data is encoded on a frequency-shift-keyed audio carrier. This signal is then decoded into data and timing control. Each command consists of a double transmission of the data word. Both words must be decoded and pass a bit-by-bit comparison before a command can be executed. Commands may be sent to the balloon from either the ground station at Palestine or from the recovery airplane.

The lower payload is suspended from the balloon by a 14-m diameter parachute. The top end of the parachute is fastened to the bottom of the balloon, and the lower payload (which contains the CIP, the battery power supplies, the terminate electronics, and the ballast) is attached to a fitting at the bottom of the shroud lines. Appropriate electrical cables and breakaway connectors are rigged in parallel with the mechanical connections. The whole bottom assembly is designed to break away from the balloon and fall to Earth while suspended from the parachute at termination of the flight.

4. FLIGHT SEQUENCE

4.1 PRELAUNCH PREPARATIONS AND LAUNCH

The balloon launchpad at the NSBF is a large circular area, 2,000 ft (600 m) in diameter. In the center of this large circle is another circular area, solidly paved, measuring 1,000 ft (300 m) in diameter. This circular launchpad allows layout of the balloon in precise alignment with the surface wind. Hay is planted in the area between the 2 circles, and a paved road surrounds the larger circle. Paved radials extend from the perimeter road toward the launchpad.

When all prelaunch preparations had been completed and the staff meteorologist had predicted favorable weather and winds at Palestine and for some 300 mi (480 km) downrange, the equipment was taken to the launch site. (Launches from Palestine are only authorized when the predicted termination point is at least 200 mi west of Palestine.)

At the launchpad, the main balloon, protected by a plastic sheath, was laid out full-length on the circular paved area. It was aligned with the direction of the wind and positioned so that the top of the balloon was on the upwind side. The top end of the balloon was passed under, then around a large, smooth, horizontal spool mounted on the front end of the launch vehicle. One end of this launching spool was hinged to the launch vehicle. The other end of the spool had a latch that could be released by a trigger mechanism. After the balloon was passed over the spool, the spool was pushed back to engage the latch so that the spool trapped the balloon. The top 10 m or so of the balloon was pulled forward from the spool, allowing the top payload to rest on the ground. It is this top 10 m of balloon that later received the helium gas during inflation. After the launching spool was latched, final preparations of the top payload began. The tow balloon was attached to the hoop with nylon lines and a final checkout of the tracker and data encoder was performed.

The launch sequence began by inflating the tow balloon with helium to the point where it just lifted the top payload assembly. The main balloon was then inflated by passing a predetermined volume of helium through 2 long fill-tubes and into the balloon. The helium formed a bubble in the part of the balloon above the launching spool. Figure 7 shows the configuration of the flight train at this stage of preparation. The balloon was launched by triggering the latch on the launching spool. When the latch was released, a stout spring caused the free end of the spool to fly forward, rotating about the hinge, which released the balloon. As the balloon rose, the second launch vehicle at the lower end of the balloon began to move forward (downwind). After the driver of the second launch vehicle had positioned the vehicle directly below the balloon and had his vehicle going along at the same speed as the balloon, he released the latch on the pin and the lower payload was released. Figure 8 shows the balloon system and the launch vehicle a few seconds after release of the launching spool just as the downwind launch vehicle began to move. As soon as the main balloon quit oscillating, a signal was sent from the launchpad that triggered the explosive charges on the ropes connected to the tow balloon. This released the tow balloon, and the launch sequence was complete.

4.2 FLIGHT

The balloons ascended at a rate of $\approx$900 ft/min (4.6 m/s) and reached float altitude after $\approx$2 hours. During the ascent, the flight controller at Palestine maintained a constant contact with ATC. Data from the onboard navigational system was continuously given to ATC so that air traffic in the area could be vectored around the balloon.

After the balloon was launched (and during flight preparation), solar cell voltages interspersed with reference calibration voltages and RTD voltages were fed into the telemetry system. These voltages were converted to PCM and were transmitted to the NSBF ground station along with the position, altitude, and other information from the CIP. At the ground station, the signals were decoded, recorded, and displayed in real time for monitoring the flight. The TV link was also used at the ground station to monitor the status of the top payload during the flight.

The first balloon was launched on June 27, 2000, at 12:48 UT (7:48 a.m. local time) and reached float altitude at 15:18 UT. The tracker was first turned on at 15:10 UT and successfully locked on the Sun. The system continued tracking and sending data until 18:15 UT, when the tracker was turned off in preparation for termination. The flight was terminated at 18:19 UT.

The second balloon was launched on July 5, 2000, at 12:20 UT (7:20 a.m. local time) and reached float altitude at 14:36 UT. The tracker was turned on and locked on the Sun at 14:33 UT. The tracker operated normally and telemetry data was received through 17:41 UT. The flight was terminated at 17:42 UT.

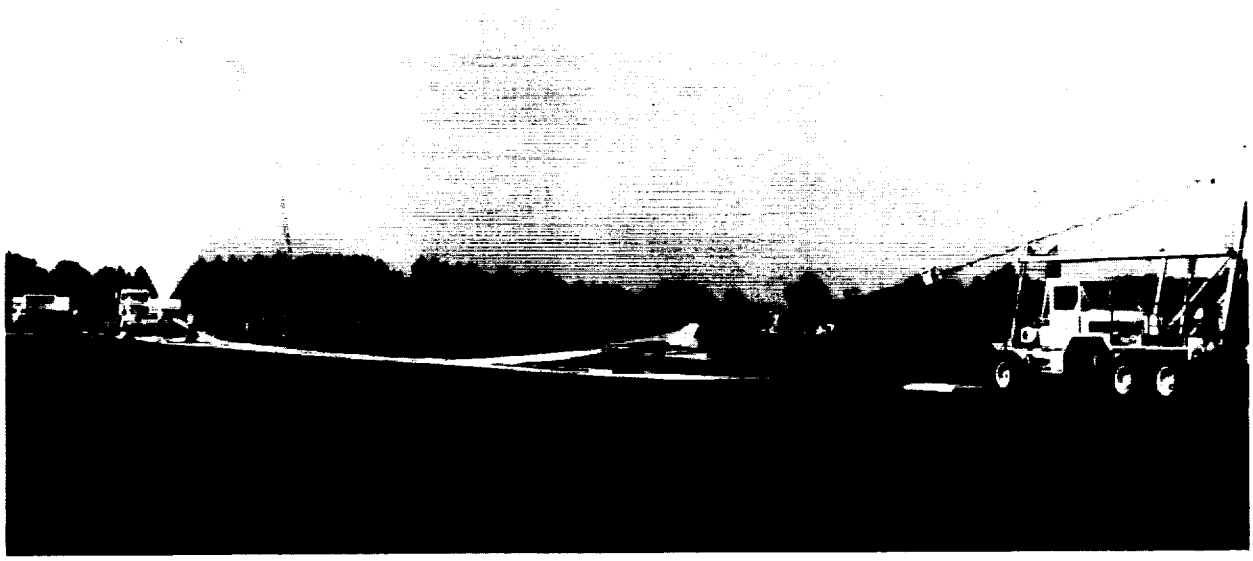

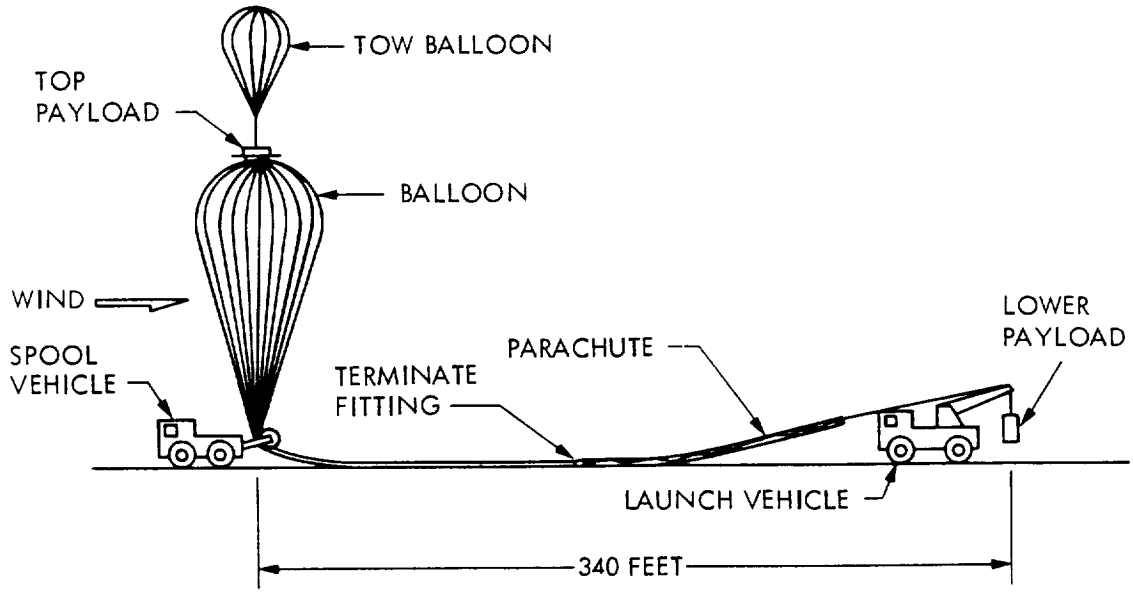

Figure 7. Flight Train Configuration

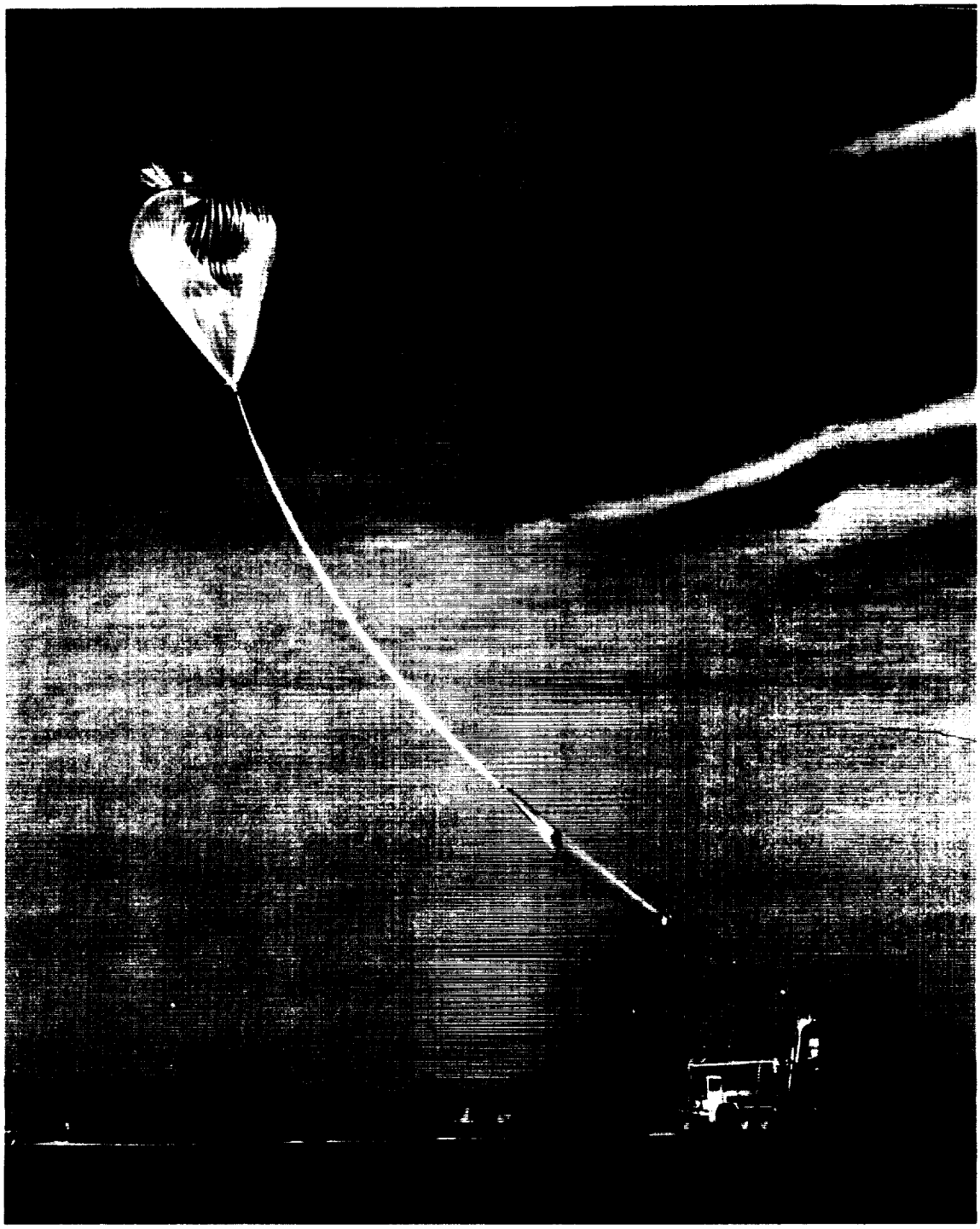

Figure 8. Balloon Launch

4.3 FLIGHT TERMINATION

Shortly after each launch, a ground recovery crew began driving toward the expected termination area in a special recovery truck. Approximately 2 hours after the balloon reached float altitude, the recovery airplane took off from Palestine with an experimenter and an observer aboard. This airplane was equipped with a telemetry receiver and a computer-controlled system that allowed the crew to monitor the location of the balloon and the status of its systems. Radio equipment aboard the airplane allowed communication with the balloon base and with the ground recovery crew. The airplane also had a full command system so that it could send commands to the balloon.

During the summer months, the winds at altitudes above 80,000 ft (24 km) blow from east to west at speeds of about 50 knots (25 m/s), so the airplane had to fly about 200 mi (330 km) west of Palestine to be in position for recovery. The pilot could fly directly toward the balloon at any time by flying toward the telemetered location of the balloon. This position information was generated by the GPS system on the balloon, telemetered to the balloon base at Palestine, and relayed from there to the airplane. The observer in the recovery airplane shared the responsibility for termination of the flight with the launch director in the NSBF control tower at Palestine. Before leaving Palestine, the recovery personnel had received a set of descent vectors from the meteorologists. The descent vectors are estimates of the trajectories that the payloads should follow as they descend by parachute. Upon receiving word that the experimenter had sufficient data, the pilot flew under the balloon to double-check the accuracy of the GPS data. Using the descent vectors, he then plotted where the payloads should come down. He also established contact with ATC. When ATC advised that the descending payloads would not endanger air traffic, and when the descent vector plots showed that the payloads would not come down in an inhabited area, the flight director at NSBF sent the commands to the balloon that terminated the flight.

The termination sequence began with a command to the balloon that disconnected power from the tracker and data encoder. Next, a command was sent that cut the cable holding the top payload onto the top of the balloon. The third command released the bottom parachute from the balloon, which allowed the bottom payload to fall away and caused the balloon to become top-heavy. As the bottom payload fell, a rip line, connected from the parachute to the body of the balloon, ripped open the side of the balloon. The balloon collapsed, the top payload fell off the balloon, its parachute opened, and all 3 objects began their descent.

Typical descent time for the top payload is $\approx$40 minutes with its present weight and with a 24-ft (7.32-m)-diameter parachute. The descent time for the bottom payload is $\approx$60 minutes. While the payloads were descending, the pilot monitored the position of the top and bottom payloads by visual reference. Both payloads were observed from the air at impact and their positions logged using an onboard GPS receiver. The ground recovery crew was directed to each impact site by the pilot as he circled the area in the airplane. This year both descents were normal, and no damage to the solar cells or to the tracker occurred.

This year the touchdown site for the first flight was near Stephenville, Texas, $\approx$150 mi (241 km) from Palestine. The total flight duration from launch until the terminate command was sent was $\approx$5.5 hours.

The touchdown site for the second flight was 5 mi. north of Blackwell, Texas $\approx$270 mi (435 km) from Palestine. Flight duration from launch until termination was $\approx$5.4 hours.

5. DATA ANALYSIS

The computer analysis was performed at JPL using a TBASIC (registered trademark of the TransEra Corp.) program written for a PC. The program read the raw data from the files produced by the LabVIEW program during the flight, then corrected the fixed-load cell data for temperature and Earth-Sun distance to a temperature of 28°C and to an Earth-Sun distance of 1 astronomical unit (AU) using the following formula:

$$V_{28,1} = V_{T,R}(R^2) - A(T - Tref)$$

where

$V_{T,R}$ = measured module output voltage at temperature T and distance R, where
R = Sun-Earth distance in AU. (See reference 2)
A = module output temperature coefficient.
T = module temperature in degrees C.
Tref = Standard temperature (usually 28°C).

A similar correction is made to the cells producing I-V curves. The correction shown above is made for all measured cell current values. A separate correction, utilizing a temperature coefficient appropriate for V_{oc}, is applied to the cell voltages, but the factor for Earth-Sun

distance is not used. This correction is made for all measured cell voltage values.

The analysis program includes the ability to compute temperature coefficients of the fixed-load cells and of the I_{sc} and V_{oc} of the I-V cells from the flight data. The cell output, corrected only for Earth-Sun distance, was used for these calculations. Data from the RTDs, mounted in 6 of the flight modules, was used for the temperature measurements. Linear least square fits to the data were used to determine the temperature coefficients. A computer-generated plot of cell output vs. temperature was useful in judging the acceptability of the temperature coefficients derived from the flight data. In most cases, the flight-derived temperature coefficients were used for the data analysis.

The program was modified in 1999 to calculate the gain of the fixed-load-cell amplifiers each time a line of data was read. The known, stable voltages from the external voltage reference source were used as input, and the telemetered output values were used in a linear least squares fit to calculate the gain and offset of the amplifiers in real time.

The program was again modified in 2000 to allow the option of calculating the gain of the fixed-load-cell amplifier using internal calibration voltages of ≈ 50 and 90 mV built into the DAQ. This option also permits calculating the gain and offset of the amplifier continuously during the flight.

The remainder of this section describes the details of performing the above corrections and computing calibration values for the cells.

5.1 DATA STREAM DESCRIPTION

The data is sent from the computer on the balloon to the ground telemetry station in groups called frames. Each frame consists of 26 lines of data, and each line contains 43 words of data. The first line of data contains the frame synch word, a line count word, a frame count word, time of day, temperature data, calibration voltages, power supply voltages, the on-Sun indicator reading, and a checksum word. The next 25 lines begin with a line synch word and a line count word. In line 2, this is followed by 30 data words corresponding to the outputs of the fixed-load cells (channels 21 through 50). Words 33 through 42 contain fill data (7s), and word 43 is a checksum. The fixed-load cell readings are repeated 4 more times and sent in lines 3 through 6 using the same format as used in line 2. Line 7 begins with the line synch word and a line count word. Words 3 and 4 contain the voltage and current readings resulting from the first load resistor applied to cell 1. The next 38 words contain the voltage and current readings for the remaining 19 loads applied to cell 1. Word 43 is again a checksum. Lines 7 through 26 contain data for the 19 I-V cells and the calibration channel in this same format. The LabVIEW program receives the data in this format and, after producing a real-time display on the computer screen, stores the data on files as it is received.

5.2 FIXED-LOAD CELLS

The computer analysis program performed its analysis in 2 steps. In the first step the cells with fixed loads were read from the files created by the LabVIEW program during the flight. The program began by looking for the frame synch word marking the beginning of a frame. Once this word was found, the on-Sun indicator reading was decoded. If this reading was greater than the minimum allowable value (OSIMIN), analysis proceeded by applying the Earth-Sun distance and temperature corrections to the data for each of the 23 fixed-load cells. Appropriate data for each cell (sums, sums of squares, number of readings, etc.) was accumulated for computing averages, standard deviations, and temperature coefficients after all the data was read.

The temperature for each cell was computed by weighting the values of the 6 RTDs (T1 through T6) on the panel. That is, if cell x was located physically on the panel midway between RTDs T1 and T2, and if T1 and T2 were both mounted under the same cell types as cell x, then the temperature for cell x would be taken to be an equally weighted average of T1 and T2. But if T1 was under a different cell type than that of cell x, then the temperature of cell x might more accurately be computed by applying a higher weighting factor to T2 than to T1. A certain amount of judgment is required of the analyst in choosing the weighting factors involved in the temperature readings. This is of some importance, since the RTDs typically show a temperature gradient over the panel of $\approx 4°C$.

The analysis of the flight data for the fixed-load cells on the first flight resulted in a minimum of 425 acceptable readings for each cell. Data points were accepted between 15:07 and 18:17 UT. The balloon remained above 118,000 ft during this time. On the second flight, data points were accepted between 14:30 and 17:40 UT, while the balloon floated above 117,000 ft. A minimum of 1,787 readings for each fixed-load cell was accepted. Averages and standard deviations were computed for each cell. The results for the 6/27/00 flight are reported in Table 1 and 3, and the results for the 7/5/00 flight are

reported in Tables 2 and 3. The cells in Table 3 are Ge cells, and the calibration values are reported for 40, 50, 60, and 70°C. These particular cells were probably somewhat shunty, causing a nonlinearity in their temperature coefficients. The load line of the installed shunt resistor intersected a part of the I-V curve that was not flat so that when the cell temperature rose and the I-V characteristic shifted left, the cell current decreased more rapidly than it would for a nonshunted cell. This made it impossible to extrapolate to the standard temperature of 28°C. In order to report a calibration value of some accuracy, we chose to use report data at temperatures where measurements were actually made. A disk with the entire set of cell readings vs. temperature was furnished to each vendor who had cells with this nonlinear characteristic.

5.3 I-V CHARACTERISTIC MEASUREMENTS

The second step in the computer analysis was to extract the data from the I-V cells. In this procedure, the frame synch word was found, then the on-Sun indicator reading and the cell temperatures, just as in the procedure for the cells with fixed loads. If the on-Sun indicator reading was at or above the OSIMIN threshold level and the Sun-angle-sensor readings were below the pointing error limits, the current-voltage pairs for each cell were read. The currents were corrected for Earth-Sun distance and for cell temperature, as described for the fixed-load cells, except that this correction was applied to every current reading using the measured temperature coefficient for I_{sc}. A correction was also made to all the voltage readings using a V_{oc} temperature coefficient appropriate for each cell, but no Earth-Sun correction was made for the voltage values. (The temperature coefficients used were usually those measured during the flight.) The application of the current and voltage corrections is equivalent to a translation in the current and voltage axes. The data for each cell was recorded on a diskette in spreadsheet-compatible format and sent to the supplier of that cell.

5.4 CALIBRATION RESULTS

Tables 1 and 2 report the calibration values of the fixed-load cells calibrated on the two 2000 balloon flights, corrected to 28°C and to 1 AU (1.496×10^8 km). Table 3 reports the calibration results of the 3 Ge cells corrected to 40, 50, 60, and 70°C and to 1 AU. The tables also report the standard deviation of the measurements, the preflight and postflight readings of each module in the X25 simulator, and a comparison of the preflight and postflight simulator readings. The simulator intensity was set with a Si standard cell. No attempt was made to match the standard cell with each module, since the purpose of the preflight vs. postflight measurements is to make sure no damage occurred to the cells as a result of the flight. The tables also report the temperature coefficients that were used for the analysis.

5.5 DATA REPEATABILITY

Several standard modules have been flown repeatedly over the 37-year period of calibration flights. Module BFS-17A, which had flown on 41 flights, was damaged in 1990 and is no longer available. In its history of 41 flights, the BFS-17A calibration values averaged 60.180, with a standard deviation of 0.278 (0.46%). In addition to giving a measure of the consistency of the year-to-year measurements, BFS-17A also provided insight into the quality of the solar irradiance falling on the solar panel, with regard to uniformity, shadowing, or reflections. This cell had been mounted in various locations on the panel over the years. Nevertheless, its readings were always consistent, which verified that there are no uniformity, shadowing, or reflection problems with the geometry of this system.

We have identified a group of solar cells that will be used as replacements for the function served by BFS-17A. Some cells from this group will be flown every year so that we can continue our year-to-year continuity checks. Six cells were flown from this continuity group on the 2000 flights. Data from these cells is presented in Table 4. Cell 73-182 was flown on the 2000 flights for the 21st and 22nd times. The calibration values, 68.20, and 68.05 were 0.44% and 0.22% higher than the average of 67.90 established over 22 flights. Two other Si cells (STS-021 and 91-004) were flown. The readings of these cells differed from the average values by +0.34% and +0.46%. These differences appear to arise primarily from the difference of temperature coefficients used in the data correction routine.

Two GaAs/GaAs cells were included in the group. One cell, 94-001, was flown for the second time. This year's reading was 0.64% higher than the value measured in 1994. The other cell, 95-002, has been measured 4 times starting in 1995. Its early repeatability was substandard and this year became even worse when its reading dropped to 16.3% below the average of the 4 flight readings. We have seen similar output decreases in GaAs/Ge balloon standard cells with time. The decrease appears to be due to a nonuniform discoloration, silvery in appearance, on the surface of the cell.

Table 1. Balloon Flight 6/27/00 118,000 ft, RV = 1.0166160 Flt. No. 1569P

MODULE CALIBRATION DATA				COMPARISON SOLAR SIMULATOR & FLIGHT				GENERAL INFORMATION
				Pre-Flt vs Post-Flt Comparison				
Module Number	Org.	Temp Intensity Adjusted Average	Std Dev	AM0, Solar Sim. 1 AU 28 Deg C. Pre-Flt	Post-Flt	Post-Flt. vs. Pre-Flt. (Percent)	Temp. Coeff. (mV/C)	Comments
00-110A	AFRL	67.80	1.1460	84.15	81.59	-3.04	0.00000	Global Solar CIGS
00-110B	AFRL	76.35	0.1158	78.84	77.33	-1.92	0.05680	United Solar amor Si
00-114	AFRL	-0.31	2.0683	83.35	81.41	-2.33	0.15900	United Solar amor Si
00-116	AFRL	64.85	0.7117	79.02	72.39	-8.39	0.00000	Global Solar CIGS
00-121	Emcore	78.14	0.0332	74.53	73.11	-1.91	0.03800	DJ Top Cell
99-131	Hughes	83.61	0.2737	80.71	79.27	-1.78	0.06500	Triple Jcn Top Irr
99-142	Hughes	84.92	0.0206	84.68	85.74	1.25	0.03990	Triple Jcn Mid (Refly)
99-143	Hughes	84.45	0.3804	80.27	80.53	0.32	-0.55030	Triple Jcn Bot (Refly)
73-182	JPL	68.20	0.0352	69.42	69.34	-0.12	0.04100	HEK 2 ohm, 14 mil (Refly)
91-004	JPL	84.70	0.0464	84.84	85.66	0.97	0.01290	ASEC 10 ohm, 8 mil (Refly)
95-002	JPL	63.80	0.0229	65.05	61.92	-4.81	-0.03540	ASEC GaAs/Ge T6
00 01A	JPL	86.45	0.0772	84.61	83.11	-1.77	0.04730	SPL TJ Top
00-01B	JPL	77.96	0.1656	76.72	78.81	2.72	0.04590	SPL TJ Mid
00-002	JPL	86.73	0.0169	85.20	83.51	-1.98	0.04160	SPL TJ Full
00-03A	JPL	87.13	0.0564	86.29	84.46	-2.12	0.04240	SPL TJ Top
00-03B	JPL	87.54	0.0295	86.16	88.91	3.19	0.03570	SPL TJ Mid
00-004	JPL	85.86	0.0203	84.49	81.67	-3.34	0.03930	SPL TJ Full
00-141A	SPL	83.34	0.1169	82.52	80.60	-2.33	0.05060	MJ Top
00-141B	SPL	83.76	0.0449	82.76	85.87	3.76	0.07320	MJ Mid
00-156	Sunpwr	82.02	0.0286	81.37	81.34	-0.04	0.03420	Si Cell
00-160	Tecstar	22.81	0.1107	21.60	21.78	0.83	-0.18410	MJ Bot
00-163	Tecstar	83.43	0.0234	83.23	83.98	0.90	0.03120	MJ Mid
00-174	TRW	80.24	0.0209	79.64	78.75	-1.12	0.04720	Sharp Si 3 mil

Table 2. Balloon Flight 7/5/00 118,000 ft, RV = 1.0167320 Flt. No. 1570P

MODULE CALIBRATION DATA				COMPARISON SOLAR SIMULATOR & FLIGHT				GENERAL INFORMATION
Module Number	Org.	Temp Intensity Adjusted Average	Std Dev	AM0, Solar Sim. 1 AU 28 Deg C. Pre-Flt	Post-Flt	Post-Flt. vs. Pre-Flt. (Percent)	Temp. Coeff. (mV/C)	Comments
00-111A	AFRL	85.22	0.0960	81.30	79.82	-1.82	0.02870	GaInP/GaAs Irr
00-111B	AFRL	80.23	0.0451	78.29	77.65	-0.82	0.06640	GaInP/GaAs Non-Irr
00-112A	AFRL	87.59	0.0704	85.12	84.17	-1.12	0.05200	SPL GaInP Top T-9
00-112B	AFRL	73.93	0.1015	74.90	74.44	-0.61	0.03850	SPL GaAs Middle M-6
00-124	Emcore	80.72	0.0629	80.12	80.37	0.31	0.01860	DJ Bottom GaAs
99-133	Hughes	77.45	0.0781	77.56	77.85	0.37	0.06420	TJ Middle Irr
99-135	Hughes	83.30	0.4076	79.55	80.09	0.68	-0.53420	Triple Jcn Bottom Irr
99-139	Hughes	83.30	0.0666	80.19	78.64	-1.93	0.03660	Triple Jcn Top
73-182	JPL	68.04	0.0432	69.42	69.36	-0.09	0.04720	HEK 2ohm-cm 14 mil
STS021	JPL	73.40	0.0733	74.47	74.67	0.27	0.05110	ASEC 2 ohm, 8 mil
94-001	JPL	80.24	0.0497	80.33	80.56	0.29	0.04950	ASEC GaAs/Ge
00-134	SPL	83.44	0.1217	84.87	85.32	0.53	0.04850	MJ Mid
00-137	SPL	79.21	0.1143	76.22	75.74	-0.63	0.05580	MJ Top
00-142A	SPL	82.01	0.0741	78.75	80.50	2.22	0.05600	MJ Top
00-142B	SPL	80.30	0.1377	81.83	82.62	0.97	0.10030	MJ Mid
00-165	Tecstar	79.81	0.0416	77.71	76.56	-1.48	0.04560	MJ Cascade Top
00-166	Tecstar	75.19	0.0429	73.03	71.93	-1.51	0.04270	MJ Cascade Full
MV1-05	TRW	91.24	0.0732	81.73	80.07	-2.03	0.10970	ASE 2PR 180 um CNES Flown
97-142	TRW	81.61	0.1376	76.01	75.32	-0.91	0.06120	USSC amor-Si
00-179	TRW	81.64	0.1273	82.44	81.99	-0.55	0.03620	Emcore TJ Full Irr 1E15
00-182	TRW	85.00	0.0426	82.64	82.55	-0.11	0.05030	Emcore TJ Full
00-185A	TRW	87.81	0.0717	84.61	84.53	-0.09	0.05290	Emcore Top
00-185B	TRW	87.42	0.1457	84.34	82.98	-1.61	0.05270	Emcore Bottom

Table 3. Solar Cells with Nonlinear Temperature Coefficients
Calibration Values at Indicated Temperatures

MODULE CALIBRATION DATA				COMPARISON SOLAR SIMULATOR & FLIGHT			GENERAL INFORMATION	
Module Number	Org.	Cell Temp. °C	Calib. Value	AM0, Solar Sim. 1 AU 28 Deg C. Pre-Flt	Post-Flt	Post-Flt. vs. Pre-Flt. (Percent)	Flight No.	Comments
99-135	Hughes	40	75.61	79.55	80.09	0.68	1570P	Triple Jcn Bottom Irr
		50	72.03					
		60	66.96					
		70	60.50					
99-143	Hughes	40	76.23	80.27	80.53	0.32	1569P	Triple Jcn Bottom (Refly)
		50	72.56					
		60	67.49					
		70	60.92					
00-160	Tecstar	40	20.24	21.60	21.78	0.83	1569P	MJ Bottom
		50	18.86					
		60	17.11					
		70	14.84					

Table 4. Repeatability of Six Standard Solar Cell Modules Over a 26-year Period

Flight Date	73-182 HEK	STS-021 Hi Blue	91-004 ASEC Si 10Ω-cm	94-001 ASEC GaAs/Ge	95-002 ASEC GaAs/Ge	95-004 ASEC Si Isc	95-004 ASEC Si Voc
4/5/74	68.37						
6/6/75	67.88						
6/10/77	67.96						
7/20/78	68.20						
8/8/79	67.83						
7/24/80	68.00						
7/25/81	67.96						
7/21/82	68.03						
7/12/83	68.03						
7/19/84	67.62						
8/84 Shuttle		73.60					
7/12/85		72.85					
7/15/86							
8/23/87							
8/7/88							
8/9/89							
9/6/90							
8/1/91			83.92				
8/1/92		73.08					
7/29/93	67.71	73.14					
8/6/94	67.77			79.75			
8/31/95	67.95				81.53		
6/30/96	67.65				79.71	166.83	617.08
8/8/96	68.26				79.53	167.49	617.90
6/11/97	67.66					168.36	614.60
8/2/97	67.53						
8/24/97	67.51					166.10	623.29
8/15/98	67.84						
6/14/99	67.79					166.0	609.1
7/6/99						166.0	596.4
6/27/00	68.20		84.70		63.80	167.0	610.6
7/5/00	68.05	73.40		80.24		166.4	610.5
No. of Meas.	22	6	2	2	4	8	8
Average	67.900	73.153	84.310	79.995	76.143	166.853	612.434
Std. Dev.	0.236	0.300	0.552	0.346	8.278	0.817	8.012
Max. Value	68.370	73.600	84.700	80.240	81.530	168.36	623.290
Min. Value	67.510	72.850	83.920	79.750	63.800	166.000	596.400
Max. Dev.	0.470	0.447	0.390	0.245	12.343	1.507	16.034

Cell 95-004, an ASEC 10 Ω-cm Si cell, is an I-V curve cell which has flown 8 times. The data for its I_{sc} and V_{oc} measurements is also shown in Table 4. The I_{sc} values are quite consistent with a standard deviation of 0.82 mA. The V_{oc} values show a larger variation with their standard deviation of 8.01 mV. We believe this arises primarily because of the variation in the temperature coefficients used in the analysis. We are refining the methods for measuring the temperature coefficients during the flight, and expect to see these variations decrease in the future.

The fixed-load cell measurements, with the exception of the degraded GaAs/Ge cell, indicate that the calibration values, using the new data acquisition system, are repeatable within themselves and consistent with measurements from previous years.

5.6 I-V MEASUREMENTS

Figures 9 and 10 are the I-V curves of JPL cell 95-004, which was flown on both 2000 flights. Figures 11 through 13 are the I-V curves of cells furnished by TRW and Figures 14 through 19 are curves of cells furnished by Spectrolab. The other I-V data is omitted by request of the sponsors. Although the I-V characteristics were measured many times during the flight, only 3 curves are shown for each cell. The curves illustrated are those corresponding to the maximum, average, and minimum values measured for P_{max}. Note that the data does not give a true measure of short-circuit current because the curves do not go through 0 volts. This is because the I-V curves are generated by a succession of resistive loads. The resistive load actually consists of a series string of resistances, including the current-measuring resistor (0.1 ohm), the leads from the DAQ to the cells and the load resistor(s) themselves. Even though the load resistance introduced by the program is 0 ohms, the remaining resistances in the string are sufficient to load the cell at a voltage considerably greater than 0 volts. This is particularly true for cells with large areas that produce large currents.

The curves are derived from the digital telemetry data recorded during each flight. Data from the Sun angle sensor was used to select only those curves taken while the tracker was pointed at the Sun to within 3° in azimuth and 2° in elevation for the first flight, and to within 3° in azimuth and between −1° and +2° for the second flight. This constraint along with the time constraints discussed above resulted in 85 acceptable I-V curves generated on the first flight and 357 acceptable curves on the second flight.

Table 5 displays some statistical data about the curves depicted in the figures. The table gives the mean, the standard deviation, the maximum measured value, and the minimum measured value for 6 of the important cell parameters. These statistics apply only to the curves that fell within the pointing accuracy criteria described above.

6. CONCLUSIONS

The 2000 balloon flights were successful. Six cells from previous flights were reflown this year. With the exception of one GaAs/Ge cell, which appears to be degrading, the 2000 measurements compared well with previous years' measurements. We believe that the agreement is very satisfactory and that the calibration values obtained from the 2000 flights can be used with a high degree of confidence.

7. REFERENCES

1. B. E. Anspaugh, R. G. Downing, and L. B. Sidwell, *Solar Cell Calibration Facility Validation of Balloon Flight Data: A Comparison of Shuttle and Balloon Flight Results*, JPL Publication 85-78, Jet Propulsion Laboratory, California Institute of Technology, Pasadena, California, October 15, 1985.

2. *The Astronomical Almanac for the Year 2000*, U.S. Nautical Almanac Office, U.S. Naval Observatory, Superintendent of Documents, U.S. Government Printing Office, Washington, DC 20402, pp. C10–C12.

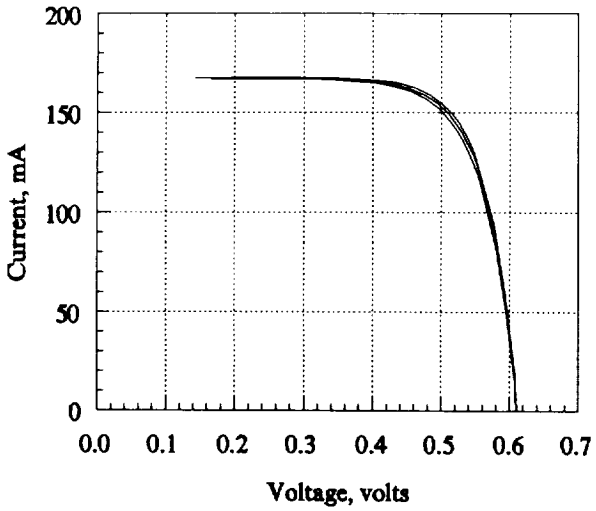

Figure 9. JPL 95-004: ASEC 10 Ω-cm, 8 mils, BSFR Flight 00-1 (1569P)

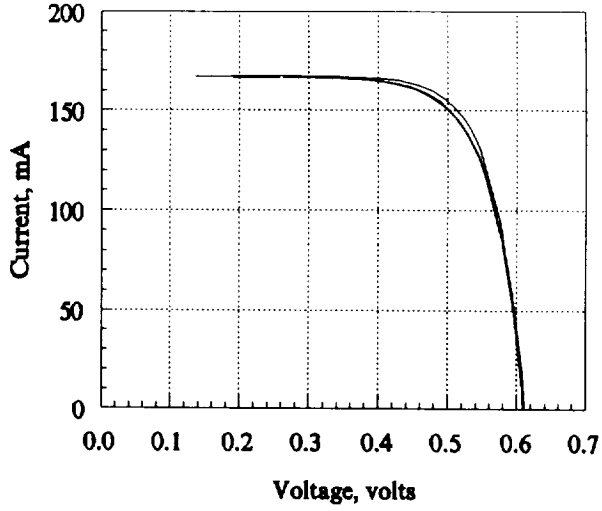

Figure 10. JPL 95-004: ASEC 10 Ω-cm, 8 mils, BSFR Flight 00-2 (1570P)

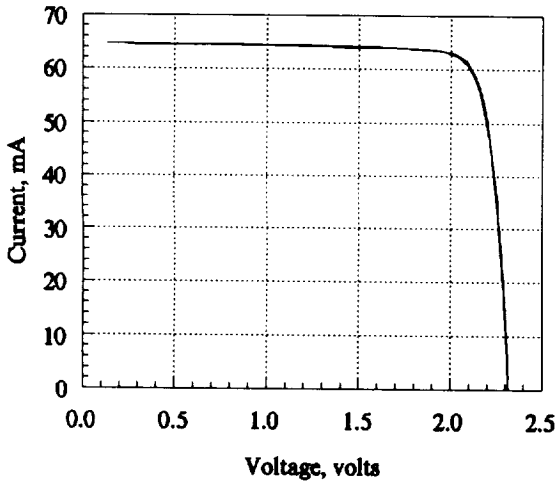

Figure 11. TRW 00-171: Emcore Full Structure Flight 00-1 (1569P)

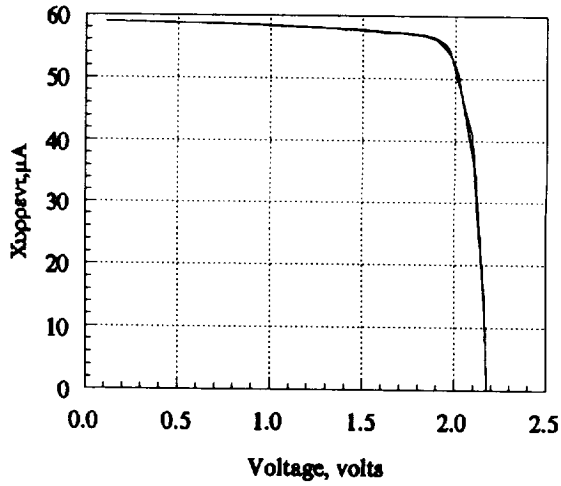

Figure 12. TRW 00-177: Emcore Dual Junction Irr 1.E15 Flight 00-2 (1570P)

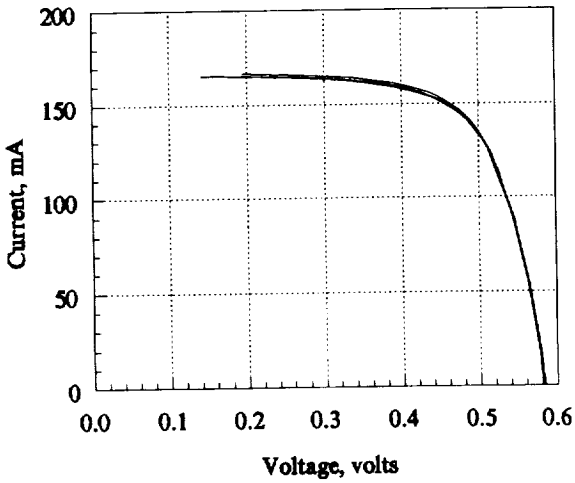

Figure 13. TRW 96-008: ASE Si 2HiR
Flight 00-2 (1570P)

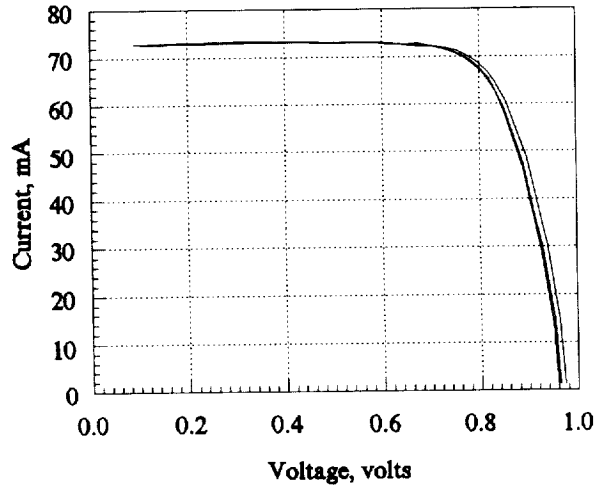

Figure 14. SPL 00-140: MJ Mid Cell
Flight 00-1 (1569P)

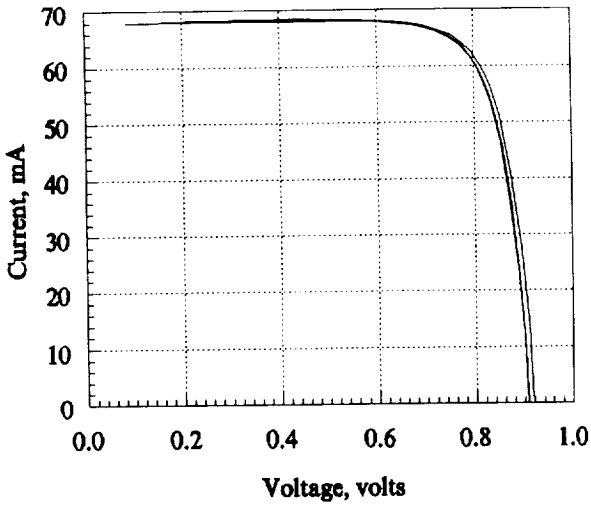

Figure 15. SPL 00-144A: MJ Mid Cell
Flight 00-1 (1569P)

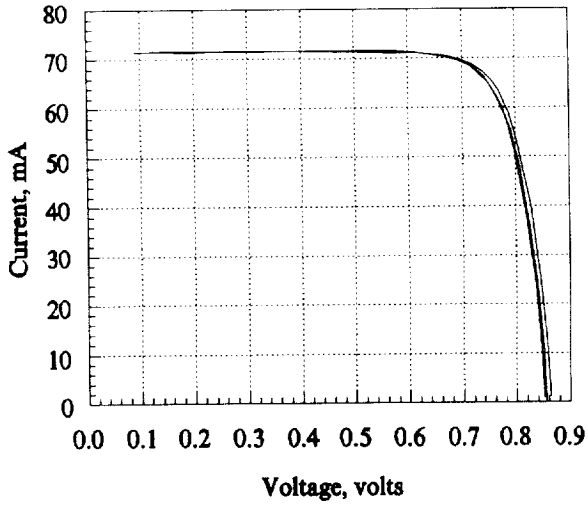

Figure 16. SPL 00-144B: MJ Mid Cell
Flight 00-1 (1569P)

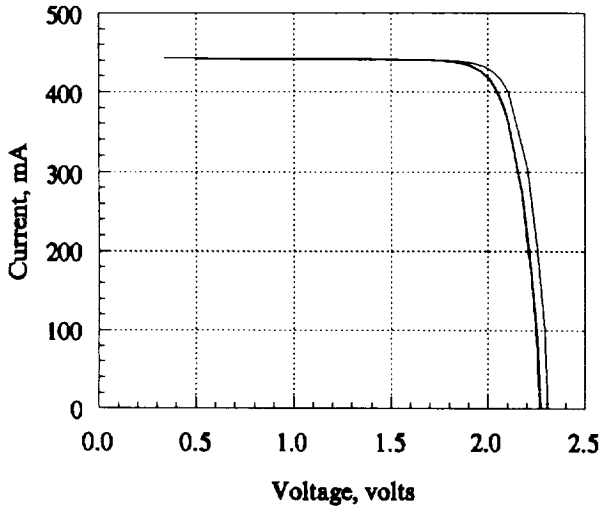

Figure 17. SPL 00-131: TJ Irr 5.E14
Flight 00-2 (1570P)

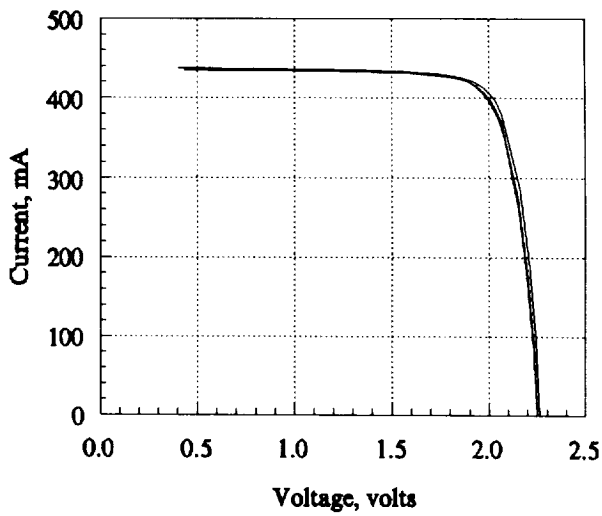

Figure 18. SPL 00-132: TJ Irr 1.E15
Flight 00-2 (1570P)

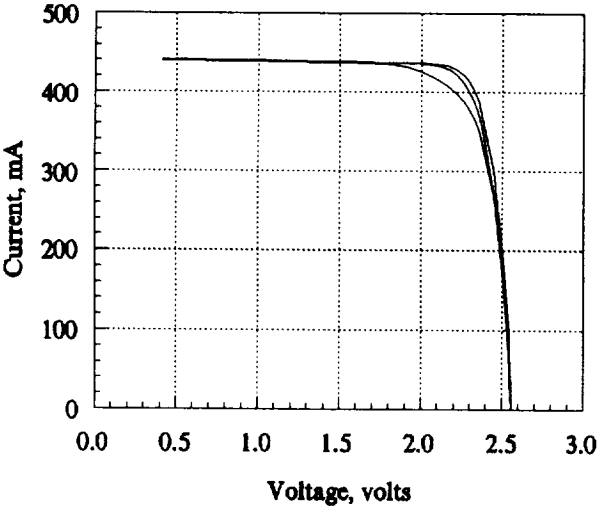

Figure 19. SPL 00-139: Triple Jcn
Flight 00-2 (1570P)

Table 5. Statistical Data for the Cells with I-V Measurements

	I_{sc}	V_{oc}	I_{mp}	V_{mp}	P_{max}	FF
95-004 (Figure 9)						
Average	167.0	610.6	153.4	495.6	76.01	0.745
Std. Dev.	0.19	0.25	1.24	4.7	0.56	0.005
Max.	167.4	611.2	155.5	506.0	77.20	0.756
Min.	167.3	610.1	149.3	489.4	75.35	0.740
95-004 (Figure 10)						
Average	166.4	610.5	153.0	494.7	75.68	0.745
Std. Dev.	0.11	0.29	1.66	6.58	0.54	0.005
Max.	166.9	611.2	155.2	511.4	77.15	0.758
Min.	166.1	609.3	148.6	487.9	75.06	0.739
00-171 (Figure 11)						
Average	64.5	2315.2	61.4	2078.8	127.61	0.854
Std. Dev.	0.07	.81	0.54	195.1	0.20	0.002
Max.	64.8	2316.6	62.9	2099.0	128.17	0.858
Min.	64.4	2312.1	60.6	2025.7	126.98	0.848
00-177 (Figure 12)						
Average	59.0	2174.7	55.3	1938.8	107.20	0.836
Std. Dev.	0.09	0.44	0.28	7.00	0.36	0.003
Max.	59.1	2176.5	56.2	1961.6	108.12	0.844
Min.	58.7	2173.4	54.7	1900.9	106.47	0.830
96-008 (Figure 13)						
Average	165.7	583.4	147.3	468.7	69.03	0.714
Std. Dev.	0.25	0.38	1.57	5.15	0.13	0.001
Max.	166.9	584.6	150.3	480.2	69.59	0.716
Min.	165.2	581.0	143.7	459.0	68.67	0.712
00-140 (Figure 14)						
Average	72.8	962.6	68.1	794.3	54.09	0.772
Std. Dev.	0.06	2.39	0.44	5.48	0.16	0.001
Max.	73.0	973.5	69.4	803.1	54.76	0.775
Min.	72.7	958.7	67.5	780.5	53.80	0.769

Table 5. Statistical Data for the Cells with I-V Measurements (Cont'd)

	I_{sc}	V_{oc}	I_{mp}	V_{mp}	P_{max}	FF
00-144A (Figure 15)						
Average	68.1	907.7	63.7	772.7	49.24	0.796
Std. Dev.	0.10	2.55	0.46	5.60	0.12	0.001
Max.	68.4	917.0	64.9	782.9	49.66	0.799
Min.	67.9	903.1	63.0	760.2	48.97	0.793
00-144B (Figure 16)						
Average	71.5	855.7	67.6	728.1	49.19	0.804
Std. Dev.	0.10	2.04	0.64	7.38	0.13	0.001
Max.	71.7	863.0	68.5	744.1	49.75	0.807
Min.	71.3	851.8	66.2	715.2	48.99	0.801
00-131 (Figure 17)						
Average	441.6	2271.0	423.9	1976.5	837.75	0.835
Std. Dev.	0.29	5.76	2.04	13.33	3.16	0.002
Max.	444.5	2312.7	426.5	2030.6	866.04	0.843
Min.	440.7	2260.0	418.5	1962.1	834.78	0.833
00-132 (Figure 18)						
Average	434.6	2251.9	408.4	1964.7	802.43	0.820
Std. Dev.	0.49	4.53	2.72	12.01	2.14	0.001
Max.	437.2	2283.3	416.7	2000.4	815.20	0.824
Min.	433.2	2245.7	404.1	1931.3	799.94	0.818
00-139 (Figure 19)						
Average	439.7	2558.1	419.4	2232.2	936.27	0.832
Std. Dev.	0.20	2.13	2.22	7.95	5.46	0.005
Max.	441.2	2567.5	426.2	2269.8	954.21	0.846
Min.	439.3	2553.4	417.3	2191.3	931.64	0.828